

Delay and distortion of slow light pulses by excitons in ZnO

T. V. Shubina¹, M. M. Glazov¹, N. A. Gippius^{2,3}, A. A. Toropov¹, D. Lagarde^{2,4},
P. Disseix², J. Leymarie², B. Gil⁵, G. Pozina⁶, J. P. Bergman⁶, and B. Monemar⁶

¹*Ioffe Physico-Technical Institute, RAS, St. Petersburg 194021, Russia*

²*LASMEA, UMR 6602, Université Blaise Pascal, 63177 Aubiere Cedex, France*

³*General Physics Institute RAS, Moscow 119991, Russia*

⁴*LPCNO, UMR INSA-CNRS-UPS, Université de Toulouse, 31077 Toulouse, France*

⁵*GES, UMR5650, Université Montpellier 2-CNRS, Montpellier, France and*

⁶*Department of Physics, Chemistry and Biology,
Linköping University, S-581 83 Linköping, Sweden*

Light pulses propagating through ZnO undergo distortions caused by both bound and free excitons. Numerous lines of bound excitons dissect the pulse and induce slowing of light around them, to the extent dependent on their nature. Exciton-polariton resonances determine the overall pulse delay and attenuation. The delay time of the higher-energy edge of a strongly curved light stripe approaches 1.6 ns at 3.374 eV with a 0.3 mm propagation length. Modelling the data of cw and time-of-flight spectroscopies has enabled us to determine the excitonic parameters, inherent for bulk ZnO. We reveal the restrictions on these parameters induced by the light attenuation, as well as a discrepancy between the parameters characterizing the surface and internal regions of the crystal.

PACS numbers: 78.20.e

The problem of optical pulse propagation in a medium has attracted attention from the beginning of the last century [1]. Loudon [2] studied the transfer of electromagnetic energy in a local dielectric with a resonant absorption line. A large number of followers [3–5] extended his analysis to include spatial dispersion. The experimental time-of-flight study of Chu and Wong [6] of a laser pulse tuned to the bound exciton (BX) line in GaP verified the prediction of Garrett and McCumber [7] on the dramatic variation of group velocity at a resonance. Their experiments promoted theoretical investigations of distortion of the temporal shape of a pulse [8–10]. Retardation of exciton-polariton propagation was studied in various semiconductors [11–13], possessing an isolated resonance, rather than an array of closely situated lines.

Renovation of the interest in slowed light was stimulated by efforts in quantum information processing [14]. That requires a delay significantly exceeding the pulse duration, while their ratio is limited by ~ 4 for quantum coherent effects [15]. The resonant optical dispersion allows one, in principle, to overcome this limit, however at the price of severe attenuation of the pulse intensity. Wide-gap semiconductors, like ZnO and GaN, promising for various optoelectronics applications, demonstrate strong excitonic resonances that makes them suitable for such a light slowing. Retardation of photoluminescence (PL) by 200 ps was observed near the 3.36-eV BX line in a 1-mm long ZnO sample [16]. In GaN, the delay was twice higher for the same sample length near BX resonances [17]. In view of these findings, the question about the distortion of a slowed pulse has been revived [18].

Here, we report on delay and distortion of light pulses by excitons in ZnO. The results are novel for two reasons: First, ZnO possesses numerous lines related to different states of donor bound excitons. The fine spec-

trum of these excitons is probed for the first time by time-of-flight spectroscopy via the local distortion of a pulse shape at different energies. Second, simulation of the general shape of the transmitted pulse permits us to determine the parameters of exciton-polariton resonances, inherent for bulk ZnO. They differ from those given by surface-probing techniques. The knowledge of correct parameters is important in many aspects; in particular, they control the delay and attenuation of a pulse.

The time-of-flight experiments were performed using the pulses of a picosecond tunable laser (Mira-HP, second harmonic). A Hamamatsu streak camera with a 2 ps temporal resolution was exploited to record the time-resolved (TR) images of the pulses. Their temporal width (~ 30 ps) was determined by instrumental accuracy. Two schemes of the measurements were exploited, which correspond to the transmission and back-scattering geometries [Fig. 1 (a), the inset]. The measurements were complemented by TR and continuous wave (cw) PL spectroscopies, as well as cw transmission and reflection measurements performed at different temperatures using a tungsten lamp. We investigated high-quality c-plane ZnO samples with the thickness L of 0.3, 0.4, 1, and 2 mm, supplied by Tokyo Denpa Co. In the PL spectra, the number (2-4) and intensity of the dominant BX lines varies among the samples, while their energies were almost identical.

The typical images of the light pulses propagating at different energies are shown in Fig. 1 (a). The leading edge of a curved light stripe, gradually narrowing due to increasing absorption, is observed up to 3.374 eV with the delay about 1.6 ns, i.e. in the close vicinity of the A exciton. Further shift of the pulse towards higher energies results in its full quenching accompanied by the increase of BX PL. In the region of relative transparency, the im-

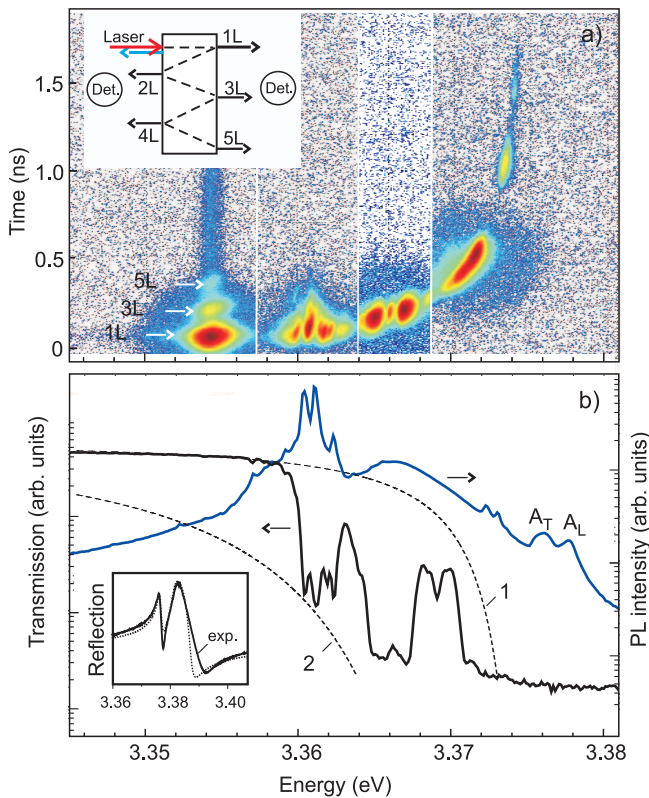


FIG. 1: (color online) (a) Combined images of four pulses propagating through the 0.3-mm sample (2 K). The boundaries between them are marked by white lines. The insert presents the scheme of signal detections, where $n \cdot L$ denote the series of replicas. (b) Spectra of cw PL, transmission, and reflection (the inset) measured in the same sample. A_T and A_L denote the transverse and longitudinal A exciton emission peaks. Dashed lines show the transmission spectra simulated neglecting the BX lines with $\hbar\Gamma_j$: 1) - 3 μeV and 2) - 30 μeV .

ages contain series of replicas, arising due to the light pulse reflection from the crystal boundaries. The mechanism of their transfer is pure ballistic [17]. They cover a distance of $n \cdot L$, where n is odd (even) number for the transmission (back-scattering) geometry. The well-defined temporal intervals between them provide a high accuracy in determination of the delays.

The images apparently show that the general curvature and delay of the pulses follow the optical dispersion controlled by the exciton-polariton resonances. The influence of the BX lines is local, namely: they provide dips cutting the pulses into several parts and induce extra light retardation nearby. Because even a very weak line can provide noticeable absorption if a sample is thick enough, the number of the BX lines resolved by the time-of-flight spectroscopy (similar to transmission) is higher than in the PL spectra [Fig. 1 (b)]. The spectral cross-sections of the pulses (Fig. 2) allow us to reconstruct the fine structure of the BX spectrum which contains at least 18 lines in the 3.356–3.374 eV range (Table I). In gen-

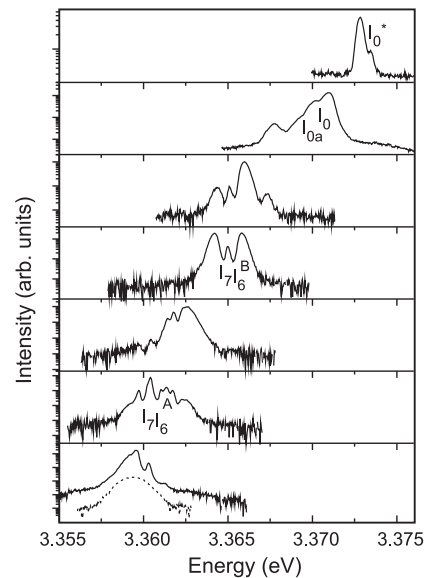


FIG. 2: Selected spectral cross-sections of the light pulses passing the 0.3-mm sample, made at different delay times from 110 ps (bottom) up to 1200 ps (top). The dips corresponding to several important lines are labelled. The initial light pulse is shown by the dotted curve.

eral, these lines can be divided into three groups: i) Two sets of A and B excitons bound to neutral donors, D^0X , separated by a gap of ~ 4.5 meV. ii) Excitons bound to ionized donors, D^+X , at higher energies. iii) Minor lines related to the vibrational-rotational (vr) states of the bound excitons. The lines of the first group produce the strongest local changes.

To model the pulse delay and distortion, the initial spectrum of the laser pulse $E = E_0(\omega)$ in the time moment t_0 is approximated as a Gaussian with the central frequency ω_0 . The amplitude and phase of the pulse are given by the Fourier transform at the boundary of a medium $z = 0$ in the linear regime. In accordance with the general theory of the electromagnetic field propagation, the electric field in the spatial point $z = L$ in the moment t can be described as [9]:

$$E(L, t) = \int_{-\infty}^{\infty} E_0(\omega) e^{ik(\omega)L - i\omega t} \frac{d\omega}{2\pi}. \quad (1)$$

Here, $k(\omega) = (\omega/c)\sqrt{\varepsilon(\omega)}$ is the complex wave vector of light, $\varepsilon(\omega)$ is the complex dielectric function of the medium.

For the medium with several exciton-polariton resonances, $\varepsilon(\omega)$ is written as: $\varepsilon(\omega) = \varepsilon_b + \sum_j X_j$, where ε_b is the background dielectric constant and X_j are the contributions of these resonances. When the resonances are assumed to be homogeneous, the expression taking into account the spatial dispersion can be readily used [20]. With inhomogeneous broadening induced, e.g., by structural imperfections, each X_j term can be represented by

TABLE I: Parameters of bound excitons in bulk ZnO obtained through the pulse distortion analysis. The notation follows Ref. [19]; X denotes unidentified lines.

Transition	E (eV)	f_{BX}	Transition	E (eV)	f_{BX}
$I_0^*(D^+X_A)$	3.3734	$5 \cdot 10^{-7}$	X	3.3635	$5 \cdot 10^{-7}$
$I_0(D^+X_A)$	3.3724	$1 \cdot 10^{-6}$	$I_6^{vr}(D^0X_A)$	3.3623	$1 \cdot 10^{-6}$
$I_{0a}(D^+X_A)$	3.3718	$1 \cdot 10^{-6}$	$I_7^{vr}(D^0X_A)$	3.3620	$1 \cdot 10^{-6}$
X	3.3705	$3 \cdot 10^{-7}$	$I_8^{vr}(D^0X_A)$	3.3616	$1 \cdot 10^{-6}$
X	3.3695	$3 \cdot 10^{-7}$	$I_5(D^0X_A)$	3.3614	$2 \cdot 10^{-6}$
X	3.3685	$1 \cdot 10^{-6}$	$I_6(D^0X_A)$	3.3608	$5 \cdot 10^{-6}$
$I_5^B(D^0X_B)$	3.3669	$1 \cdot 10^{-6}$	$I_7(D^0X_A)$	3.3600	$5 \cdot 10^{-6}$
$I_6^B(D^0X_B)$	3.3653	$2 \cdot 10^{-6}$	$I_8(D^0X_A)$	3.3593	$5 \cdot 10^{-9}$
$I_7^B(D^0X_B)$	3.3647	$2 \cdot 10^{-6}$	$I_9(D^0X_A)$	3.3566	$1 \cdot 10^{-9}$

the convolution of the line with the Gaussian centered on the same frequency [17]:

$$X_j = \int \frac{f_j \omega_{0,j}}{\omega_{0,j} + \beta k^2 + \xi - i\Gamma_j - \omega} \frac{1}{\sqrt{\pi} \Delta_j} \exp\left(\frac{-\xi^2}{\Delta_j^2}\right) d\xi. \quad (2)$$

Here, each j resonance is characterized by a frequency $\omega_{0,j}$, an oscillator strength f_j , and a damping term Γ_j . Δ_j describes the inhomogeneous width. Spatial dispersion is taken into account by the term $\beta k^2 = (\hbar^2/2M_j)k^2$, where the effective masses M_j are assumed to be infinite for BX and equal $0.9m_e$ for each free exciton resonance. Equations (1) and (2) allow for the spatial dispersion in a simplified way, they are valid for ω not too close to $\omega_{0,j}$, which is sufficient for our purposes. The pulse shapes are calculated from (1) by means of the Wigner transform.

In our simulations, all noticeable BX lines were taken into account. The $\hbar\Gamma = 1 \mu\text{eV}$ and $\hbar\Delta = 75 \mu\text{eV}$ characterize these narrow lines. The f_{BX} values corresponding to the observed local distortion are given in Table I. For the sake of illustration, we present the modelling of the intricate pattern appearing when the central energy of the pulse falls to the gap between the closely situated I_6 and I_7 lines. The light propagates there as an extremely narrow ~ 0.3 meV stripe [Fig. 1 (a)]. Figure 3 shows that a twice higher f value taken for the D^0X_B transitions ($4 \cdot 10^{-6}$ vs $2 \cdot 10^{-6}$) provides an unacceptably long delay and too strong distortion of the pulse.

To determine the parameters of the exciton-polariton resonances, we consider exclusively the data on the processes taking place inside the crystal, namely: cw transmission and pulse propagation. We abstain from using the data of reflection and PL spectroscopies, because they probe mostly a region close to the surface. The modelling is simplified owing to the fact that each excitonic parameter is responsible predominantly for a particular characteristic. For instance, the oscillator strength controls the overall curvature of a pulse via the variation of the group velocity $v_g(\omega) = d\omega/dk$ and, hence, the dif-

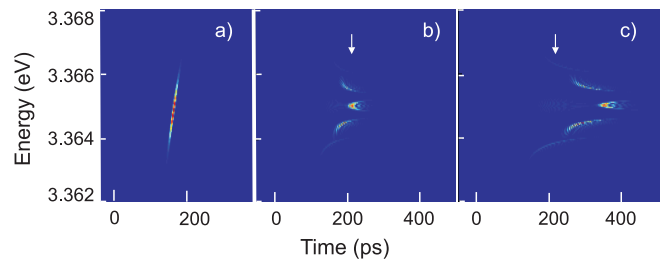


FIG. 3: (color online) Simulations of the shape of the 5-ps pulse centered at 3.365 eV propagating through the 0.3-mm sample: (a) assuming no BX lines; (b,c) taking into account the BX lines with (b) $f = 2 \cdot 10^{-6}$ and (c) $f = 4 \cdot 10^{-6}$. Arrows mark the experimental delay of the pulse center.

ferent delay $T = L/v_g$ of the pulse constituents. The derived exciton-polariton parameters are collected in Table II (the distant C exciton is neglected).

The modelling reveals two severe limitations:

1) The damping term $\hbar\Gamma$ must be as small as $\sim 3 \mu\text{eV}$. Higher values would result in the full opaqueness in the transmission spectra in the range where the narrow BX lines are clearly resolved [Fig. 1 (b)]. This is independent on the model used to describe $\varepsilon(\omega)$, because the absorption depends on the imaginary part of the dielectric function, which is determined by this term.

2) The inhomogeneous width $\hbar\Delta$ cannot exceed 0.5 meV for the A exciton resonances. This restriction arises from the observation of the transmitted light at 3.374 eV. With stronger broadening, which may occur in crystals of worse quality or with a temperature rise, the pulse propagating at this energy would be attenuated up to full disappearance. The pulse maximum can be at lower energy due to enhanced absorption at the leading edge.

The critical value of the effective damping parameter, yet maintaining the polaritonic modes [21], is $\hbar\omega_0(4f_j\hbar\omega_0/Mc^2)^{1/2} \sim 1.6$ meV in ZnO for the A exciton, being close to the longitudinal-transverse splitting

TABLE II: Exciton-polariton parameters derived from the volume- and surface-probing measurements.

Parameter	A exciton	B exciton
<i>TR and cw transmission</i>		
$\hbar\omega_0$ (eV)	3.376 ± 0.0002	3.382 ± 0.001
f	0.0072 ± 0.0002	0.012 ± 0.001
ω_{LT} (meV)	~ 3	~ 5
$\hbar\Gamma$ (μeV)	3 ± 0.2	3.5 ± 0.5
$\hbar\Delta$ (meV)	< 0.5	< 1
<i>PL and reflection</i>		
$\hbar\omega_0$ (eV)	3.3758 ± 0.0002	3.382 ± 0.001
ω_{LT} (meV)	1.8 ± 0.2	6.5
$\hbar\Gamma^*$ (meV)	0.75	1.5

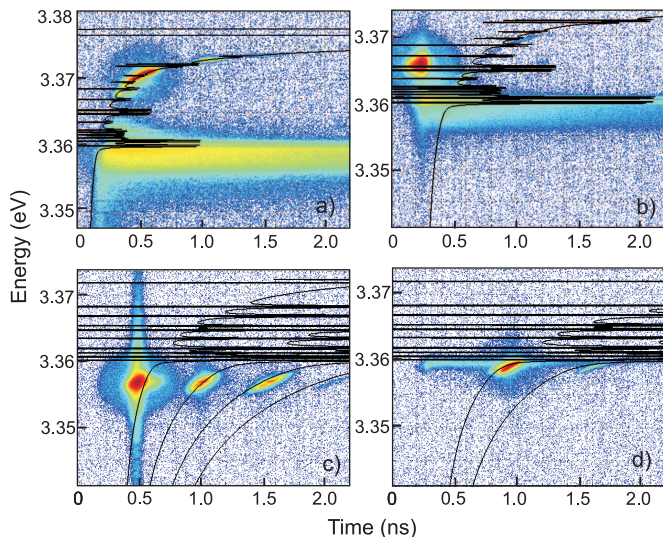


FIG. 4: (color online) Light pulses propagating through the 0.3-mm (a,b) and 1-mm (c,d) samples. The registration is done at 2 K in the transmission (a,c) and back-scattering (b,d) geometries. The black lines present the delay dependencies calculated taking into account the BX transitions.

ω_{LT} [22]. Our constraints based on the signal attenuation are more rigorous. In fact, they do not exclude that the excitonic resonances inside the crystal are homogeneous with $\hbar\Gamma$ of a few μeV . With these limitations, we have simulated the TR images of the pulses of different energies and the series of replicas, using the same exciton-polariton parameters for all samples (Fig. 4).

Our modelling has revealed obvious contradiction between the results of volume- and surface-probing experiments (Table II). The set of the parameters, perfectly fitting the cw and TR transmission data, results in too sharp peaks in the simulated spectra of reflectivity. The successful fitting of the spectrum in Fig. 1 (b), using the model of the homogeneous resonances [20], requires the empirical damping term $\hbar\Gamma_A^* = 0.75$ meV. Similar result can be obtained assuming the resonances as inhomogeneous with $\hbar\Delta_A \sim 0.9$ meV. However, both variants would provide too strong attenuation of the propagating light. Further, the splitting between the PL peaks, ascribed to transverse and longitudinal A exciton emission, is 1.6 – 2 meV, whereas the rough estimation using the bulk parameters gives $\omega_{LT} \approx 3$ meV. There are differences in the resonance energies as well. This dependence on the measurement technique is suggestive of certain broadening and deterioration of the excitonic resonances at the surface, which can be induced by modified structural properties and local electric fields [23, 24].

In conclusion, our studies exhibit that a strong resonant delay (up to 1.6 ns) of light pulses in ZnO is accompanied by their severe attenuation and shape distortion. Simulation of the shapes enables us to determine the excitonic parameters, inherent for bulk ZnO, and to estab-

lish that the resonances must have the low damping (~ 3 μeV) and limited broadening to allow the light propagation. We believe that this paper will draw attention to the time-of-flight spectroscopy as a new opportunity to investigate the fine structure of BX spectrum. The discrepancy between the surface and volume parameters implies that only the processes taking place inside the crystal, like the pulse propagation, are suitable to give the true bulk characteristics.

This work has been supported in part by the RFBR, the Program of the Presidium of RAS, and the Dynasty Foundation. TVS acknowledges the Université Montpellier 2 for its hospitality.

-
- [1] For a review, see L. Brillouin, *Wave propagation and group velocity* (Academic, New York, 1960).
 - [2] R. Loudon, *J. Phys. A* **3**, 233 (1970).
 - [3] M. A. Bishop and A. A. Maradulin, *Phys. Rev. B* **14**, 3384 (1976).
 - [4] A. Puri and J. L. Birman, *Phys. Rev. Lett.* **47**, 173 (1981).
 - [5] S. V. Branis, K. Arya, and J. R. Birman, *Phys. Rev. B* **39**, 8371 (1989).
 - [6] S. Chu and S. Wong, *Phys. Rev. Lett.* **48**, 738 (1982).
 - [7] C. G. B. Garrett and D. E. McCumber, *Phys. Rev. A* **1**, 305 (1970).
 - [8] M. D. Crisp, *Phys. Rev. A* **4**, 2104 (1971).
 - [9] L. A. Vainshtein, *Sov. Phys. Uspekhi* **19**, 189 (1976).
 - [10] P. Halevi and R. Funchs, *Phys. Rev. Lett.* **55**, 338 (1985).
 - [11] D. Fröhlich, A. Kulik, B. Uebbing, A. Mysyrowicz, V. Langer, H. Stolz, and W. von der Osten, *Phys. Rev. Lett.* **67**, 2343 (1991).
 - [12] M. Kuwata, T. Kuga, H. Akiyama, T. Hirano, and M. Matsuoka, *Phys. Rev. Lett.* **61**, 1226 (1988).
 - [13] T. Godde, I. A. Akimov, D. R. Yakovlev, H. Mariette, and M. Bayer *Phys. Rev. B* **82**, 115332 (2010).
 - [14] M. Bigelow, N. Lepeshkin, and R. Boyd, *Science* **301**, 200 (2003).
 - [15] A. Kasapi, M. Jain, G. Y. Yin, and S. E. Harris, *Phys. Rev. Lett.* **74**, 2447 (1995).
 - [16] G. Xiong, J. Wilkinson, K. B. Ucer, and R. T. Williams, *J. Phys.:Condens. Matter* **17**, 7287 (2005).
 - [17] T. V. Shubina, M. M. Glazov, A. A. Toropov, N. A. Gippius, A. Vasson, J. Leymarie, A. Kavokin, A. Usui, J. P. Bergman, G. Pozina, and B. Monemar, *Phys. Rev. Lett.* **100**, 087402 (2008).
 - [18] D. S. Wiersma, *Nature* **452**, 942 (2008).
 - [19] B. K. Meyer, J. Sann, S. Eisermann, and S. Lautenschlaeger, *Phys. Rev. B* **82**, 115207 (2010).
 - [20] J. Lagois, *Phys. Rev. B* **16**, 1699 (1977).
 - [21] M. Matsushita, J. Wicksted, and H. Z. Cummins, *Phys. Rev. B* **29**, 3362 (1984).
 - [22] C. Klingshirn, J. Fallert, H. Zhou, J. Sartor, C. Thiele, F. Maier-Flaig, and H. Kalt, *Phys. Status Solidi B* **247**, 1424 (2010).
 - [23] J. Lagois, *Phys. Rev. B* **23**, 5511 (1981).
 - [24] B. Monemar, P. P. Paskov, J. P. Bergman, G. Pozina, A. A. Toropov, T. V. Shubina, T. Malinauskas, and A. Usui, *Phys. Rev. B* **82**, 235202 (2010).